Comparative Study on Mental Stress Assessment from ECG Signal Using Detrended Fluctuation and Recurrence Quantification Analysis

MD. IMTIYAJ SHARIF[1], MD. AZIM KHAN[2], AINUL ANAM SHAHJAMAL KHAN[3]
Department of Electrical and Electronic Engineering
Chittagong University of Engineering and Technology
Chittagong-4349
BANGLADESH
gazisharifeeecuet@yahoo.com[1], azimkhaneee@yahoo.com[2], khanshahjamal@yahoo.com[3]

Abstract: - This paper presents a comparative study on the evaluation of mental stress between two groups of subjects. Mental stress influences the activity of the autonomic nervous system (ANS) which again controls the heart rate variability (HRV) signal obtained from the ECG signal. Among the subjects, group 1 contains the ECG data recorded from the students who are not examinee, while group 2 represents the students who are examinee. An ECG measurement system has been designed and implemented, by which the ECG signals from 36 university students have been recorded for 30 minutes long time. The raw ECG signal is usually contaminated by the different types of noises. Consequently, digital FIR filter has been implemented to denoise the noisy ECG signal and an algorithm has been developed in order to extract the R-R interval series. The R-R interval series undergoes the detrended fluctuation analysis (DFA) and the recurrence quantification analysis (RQA), yielding the parameters of the respective methods. Finally, the performance of the two methods on the mental stress assessment is determined by making the ANOVA test on the parameters, which shows that the RQA parameter exhibits a significant result within the level of significance ($p = 0.05$).

Key-Words: - Mental stress, ECG measurement, digital FIR filter, R-R interval series, detrended fluctuation analysis (DFA), recurrence quantification analysis (RQA), ANOVA test.

1 Introduction

Stress is one of the serious health consequences in present society as it is responsible for about half of the work related illness [1]. Mental stress may be defined as any uncomfortable feeling or emotional experience under abnormal pressure [2]. The autonomic nervous system (ANS) is divided into the sympathetic and parasympathetic nervous system, which modulates the activity of the cardiac muscle by controlling the sinoatrial (SA) node of the heart. Under stressful situation, the sympathetic nervous system causes the body to respond to stress, resulting a fight-flight response. The body cannot keep this state for long periods of time and parasympathetic nervous system counterbalances the effect of the sympathetic activity and restores the body to the normal state [2], [3]. Under normal situation, a balance is established between these two activities. However, under stressful situation, this balance will be changed and analysis of the heart's electrical activity could follow the change in the balance of the two systems [2].

The electrocardiogram (ECG) is the recording of electrical activity of the heart's muscle [4]. A typical ECG waveform consists of different waveforms (P, Q, R, S, and T) as shown in Fig.1.

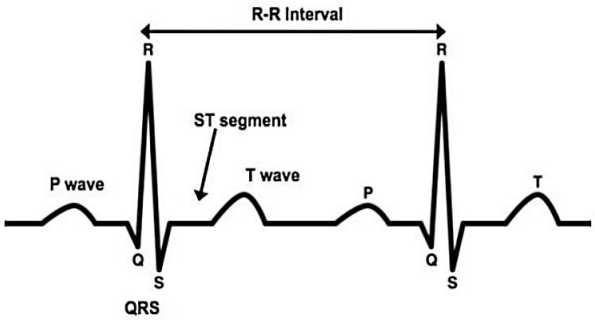

Fig.1: R-R interval of an ECG signal [3]

The time duration between the consecutive R points is known as the R-R interval time series or inter-beat interval (IBI). The reciprocal of each R-R interval in minutes is called the Instantaneous Heart Rate (IHR). After interpolating and resampling the Instantaneous Heart Rate, the Heart Rate Variability (HRV) signal is obtained [5]. The heart rate changes over time with no linear relationship between HR and time, thereby resulting a complex and nonlinear mechanism of

heart rate control. Therefore, many approaches have been developed in order to analyse the nonlinear or dynamic behaviour of the R-R interval series [6].

2 Literature Review

During the late twentieth century and early twenty-one century, different analysis methods and algorithms were developed in order to process the signal, analyse, classify and obtain a significant result with better efficiency. Some important classifying methods include digital signal analysis, Fuzzy Logic Methods, Artificial Neural Network, Hidden Markov Model, Genetic Algorithm, Support vector Machines, Selforganizing Map etc. [7].

This section reflects some recent researches on the assessment of mental stress from the ECG signals. In 1998, Wang., F., K. Sagawa, and H. Inooka developed a simple time domain HRV analysis for assessment of dynamic changes of stress [8]. In 2007, Mohit Kumar et al. presented a novel HRV analysis technique for mental stress assessment using fuzzy clustering. They also used a robust identification technique in order to handle the uncertainties due to individual variations for the assessment of mental stress [9]. In 2008, Kim., Desok, et al. investigated time dependent variations of HRV features in order to detect subjects under chronic stress. In 2010, Nagae, Daisuke and Atsushi Mase introduced two robust signal processing techniques for stress evaluation using microwave reflectometric cardiopulmonary sensing instrument. In 2011, Boonnithi, Sansanee, and Sukanya Phongsuphap measured various HRV features for detecting mental stress by using ultra short term HRV analysis [8]. D. P. Goswami, D. N. Tibarewala, and D. K. Bhattacharya used second order difference plot in order to analyze the heart rate variability to differentiate the meditative from the non-meditative condition. It was found that in meditation, the axis of elliptical cluster rotated anticlockwise from the cluster formed from the premeditation data, although the amount of rotation differs in every case [10]. In 2012, Mohit Kumar et al. suggested a stochastic fuzzy analysis method to evaluate the short time series of R-R intervals (time intervals between consecutive heart beats) for a quantification of the stress level [11]. In 2013, Vikas Malhotra1, Mahendra Kumar Patil performed statistical analysis of bio-orthogonal wavelet coefficients for the assessment of mental stress. They also trained a back propagation neural network in order to classify the stress level [2]. In 2014, D'addio, G., et al. developed a nonlinear measures of HRV during ECG stress test based on typical properties of chaotic systems and deterministic fractal [8]. In this paper, a comparative study has been performed on the mental stress evaluation using a recent recurrence quantification analysis (RQA) and an old detrended fluctuation analysis (DFA) methods. Finally, a statistical ANOVA test is accomplished on the results of the two methods which shows a superiority of RQA over the DFA method.

3 Methodology

The complete methodology of the work can be divided into two sections which can be named as (1) ECG Instrumentation System and (2) Processing and Analysis of the Recorded data.

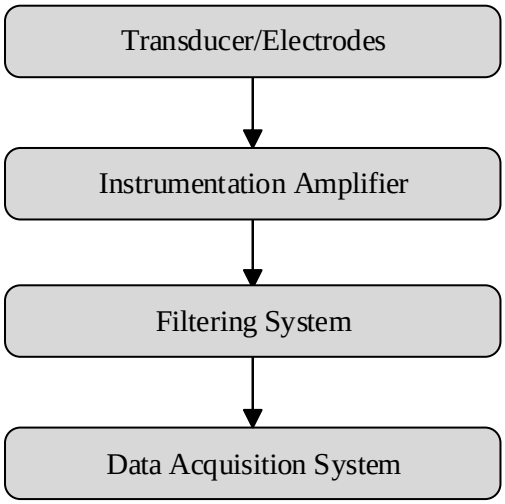

Fig.2: Block Diagram of the ECG data recording system

Above 36 subjects who are university students have participated in this projects. However, excluding the highly corrupted data, 36 healthy data have been selected for the analysis purposes. These data have been recorded over two groups based on the condition of the subjects (either examinee or non-examinee) and saved in '.mat' format via computer software & Program. The complete ECG data recording process is shown in Fig.2.

Fig.3 presents the sequence of the data processing (denoising & feature extraction) and analysis of the data in order to make a decision on the results of the methods obtained from the two groups.

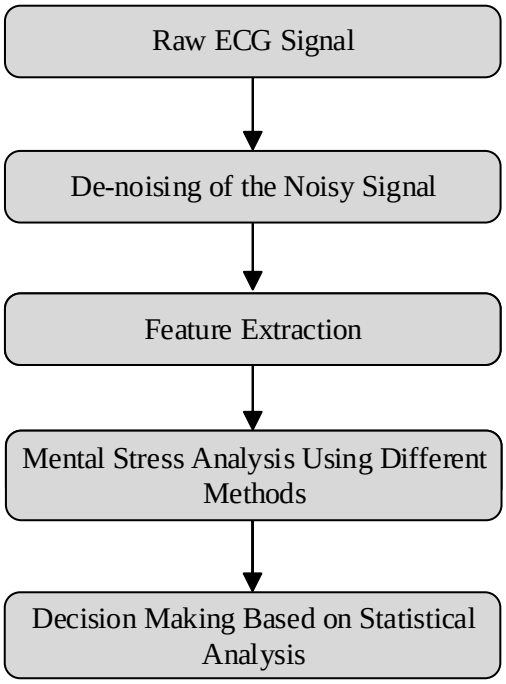

Fig.3: Block diagram showing the process of data analysis for mental stress assessment

4 The ECG Instrumentation System

The bio-potentials automatically generated by the assembly of the cardiac cells possess a very low amplitude. Consequently, the signal to be recorded are also small in amplitude (usually, in the range of 1mV to 3mV). These signals have frequency range in the value of 0.05 Hz to 100 Hz. or cycles per second [12]. Based on these requirements, there are three main aspects of the ECG measurement circuit to be designed: the skin-to-circuit interference, the amplifier circuit, and the filtering circuit. The ECG measurement information is sensed by electrodes affixing at some particular locations on the surface of the body. The signal is then amplified by the properly designed instrumentation amplifier. In order to remove the influence of noise and interference, it is necessary to design the filter circuits with desired frequency range and other circuitry. The signal can be visualized in oscilloscope or connected to a recorder or PC to collect and analyse. The complete ECG recording process is shown in Fig.4.

Electrodes works as a transducer which converts physical signal into electrical voltage (usually in the range of 1mV to 5mV). In this work, Wilson Electrode System is used. This system uses 'the Lead I configuration' and 'the RL lead' as 'the driven right leg lead' (DRL).

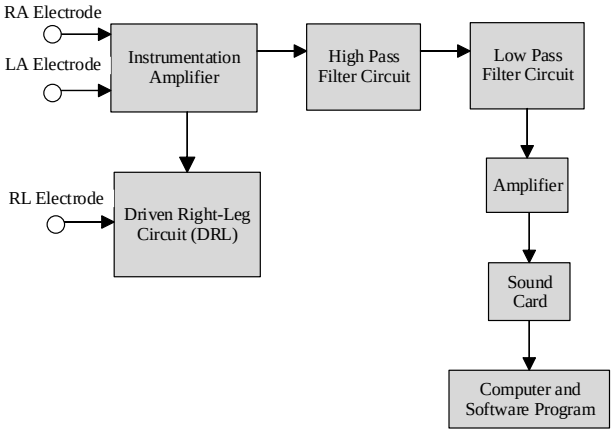

Fig.4: Block Diagram of ECG Measurement System

An instrumentation amplifier (in-amp) is a type of differential amplifier that amplifies the difference between the two input signal voltages while rejecting any signals that appear to both of the input terminals. Thus, the in-amp performs the very important function of extracting the small signals in the presence of large common mode voltages and DC potentials. In this work, the AD620 which is the low cost, low power, high accuracy instrumentation amplifier with CMMR greater than 100 dB has been used [13]. The gain of the in-amp can be set only by one external resistor (R_G) according to the following equation:

$$R_G = \frac{49.4k\Omega}{G-1} \quad (1)$$

This Driven Right Leg (DRL) Circuit provides a reference point for the patient that is normally at the ground potential. The output of the DRL circuit is connected to the electrode on the patient's right leg. The common mode voltage on the body is sensed by the two averaging resistors Ra, connected to the two terminals of the gain resistor (R_G) of AD620 and inverted, amplified, fed back to the right leg as shown in Fig.5. This negative feedback drives the common mode voltage to a low value. The body's displacement current flows not to ground rather to the op-amp output of the DRL circuit. This reduces the interference and effectively ground the patient. The DRL circuit also provides some electrical safety to the patient. If the op-amp saturates due to abnormal high voltage appearing between the patient and ground, a high resistance path occurs to the ground which limits the flow of large currents [14]. A low pass filter with cut off frequency of 160 Hz has been designed in order to maintain the stability of the driven leg loop.

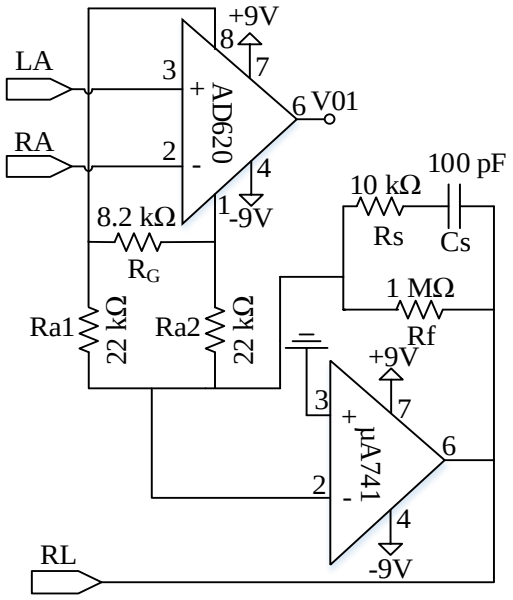

Fig.5: The instrumentation amplifier and the driven right leg (DRL) circuit

As the lower frequency limit of the ECG signal at the output of the AD620 is about 0.05 Hz, a high pass filter with the cut off frequency of 0.6 Hz has been designed.

The cut off frequency of a filter is given as

$$f_c = \frac{1}{2\pi RC} \tag{2}$$

In this circuit, we have used the second order (two pole) active filter called 'Sallen-Key-Filter" which provides roll-off rate of -40 dB/decade compared to the first order filter with roll-off rate of -20 dB/decade, [15] as shown in Fig.6.

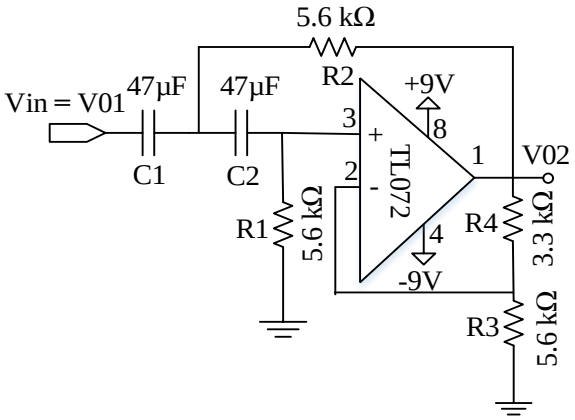

Fig.6: The 'Sallen-Key' high pass filter circuit

As the upper limit of the ECG signal is about 100 Hz, the cut off frequency of the second order low pass filter is designed as about 100 Hz using equation 2. Fig.7 shows the designed 2nd order low pass filter.

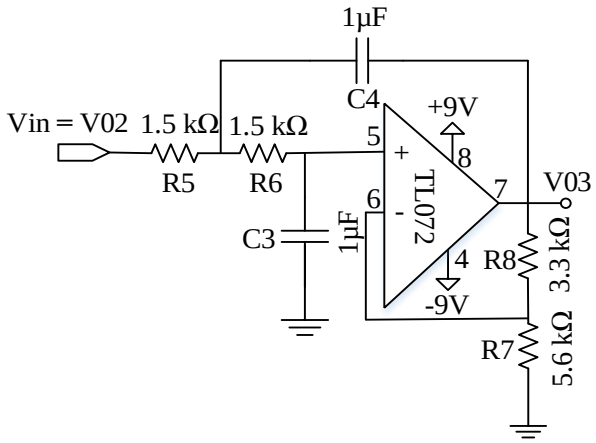

Fig.7: The 'Sallen-Key' low pass filter circuit

In order to limit the output voltage obtained from the low pass active filter within the safe level of the sound card, an additional operational amplifier (Fig. 8) is used in the final stage to set the gain at the desired value. The gain of the non-inverted operational amplifier is given by the following equation

$$A_v = 1 + \frac{R_{10}}{R_9} \tag{3}$$

As output voltage from the instrumentation amplifier is about 0.03 V, in order to have a output voltage within the range of 1 V, the gain of the operational amplifier (*Av*) should be chosen below 1/0.03 = 33 to avoid any damage of the sound card from the high voltage. The ECG signal from the sound card is recorded with 1000 Hz sampling frequency via a data acquisition algorithm developed in MATLAB software.

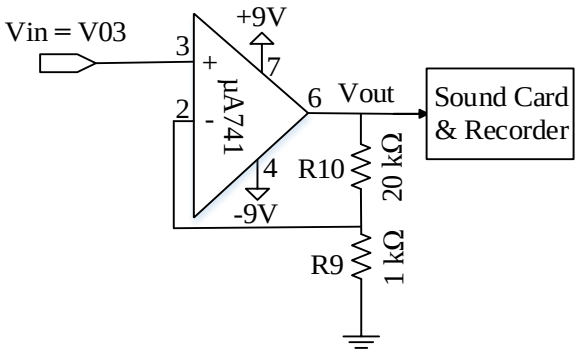

Fig.8: The operational amplifier and the data recording system

Design:

Given, V_{in} = 5 mV.

Let, R_G =8.2 kΩ, then from equation 1,

$$G = 1 + \frac{49.4 \times 10^3}{8.2 \times 10^3} = 6.$$

Then, the output voltage of the AD620 stands as

$V_{01} = G \times V_{in} = 0.03$ V

Let, $R_f = 1$ MΩ and $R_a = R_{a1} = R_{a2} = 22$ kΩ.

Then, the typical gain of the DRL circuit becomes,

$$G = -\frac{2R_f}{R_a} = \frac{2 \times 1 \times 10^6}{22 \times 10^3} = 90$$

Let, the cut off frequency of the high pass filter, f_{ch} = 0.6 Hz and choose, $R_1 = R_2 = 5.6.k\Omega$,then from equation 2,

$$C_1 = C_2 = \frac{1}{2 \times \pi \times 0.6 \times 5.6 \times 10^3} = 47 \text{ uF}$$

Let, the cut off frequency of the low pass filter, f_{cl} = 100 Hz and choose, $R_1 = R_2 = 1.5\,k\Omega$, then from equation 2,

$$C_1 = C_2 = \frac{1}{2 \times \pi \times 100 \times 1.5 \times 10^3} = 1\,uF$$

For butterworth response with a flat response in the pass band and roll of rate of -20/decade/pole, the damping factor, DF is 1.414 which is given by the following formula: $DF = 2 - \frac{R_4}{R_3}$, then choosing, R_3 = 5.6 kΩ gives R_4 = 3.3 kΩ.

In order to limit the output voltage below 1V, choosing R_9 =1 kΩ, equation 3 gives the maximum value of R_{10} = 20 kΩ.

5 Processing and Analysis

The raw (recorded) ECG signal is inherently contaminated due to the influence of noises from various sources into the analog circuitry. Therefore, it is necessary to identify the frequency band of the noises corrupting the ECG signal and develop some filtering techniques to remove these noises [16]. Besides, an algorithm has been developed in order to detect the R-peaks and hence extract the R-R time series. The R-R interval series is then analysed using DFA and RQA methods for comparative study on mental stress.

The ECG signal processing can be divided into two stages by functionality, [12]:

- Pre-processing stage
- Feature Extraction stage

5.1 Pre-processing

The common ECG contaminants may classified in to the following categories:

- Power line interference.
- Electrode pop or contact noise.
- Patient electrode motion artifacts.
- Electromyography noise.
- Baseline wandering
- Instrumentation noise generated by analog electronic devices.

Among these contaminants, the power line interference and the baseline wandering is prominent and can interrupt the analysis of the signal. The power line interference coming from the electric power system is the main source of noise in most bio-electric signal. This signal is a narrow-band noise centered at 50 Hz with a bandwidth of less than 1 Hz. Baseline wandering usually comes from respiration at frequencies wandering between 0.15 and 0.3 Hz. Besides, there may also be introduced some unwanted high frequency noise which may distort the signal [12], [17]. In this study, in order to remove these noises, we have used the Digital FIR filter structures (Fig.9) as FIR filter exhibits stable and exactly linear phase response.

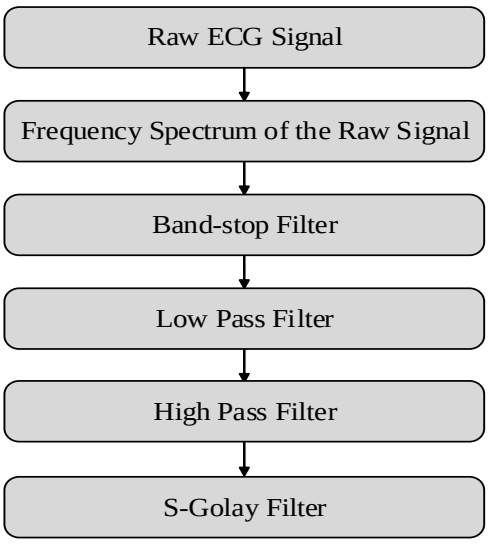

Fig.9: Block diagram showing the de-noising process by MATLAB program

This frequency spectrum shows what types of noise are available in the raw signal (Fig.10). The frequency spectrum is computed by an algorithm developed using the Fast Fourier Transform (FFT).

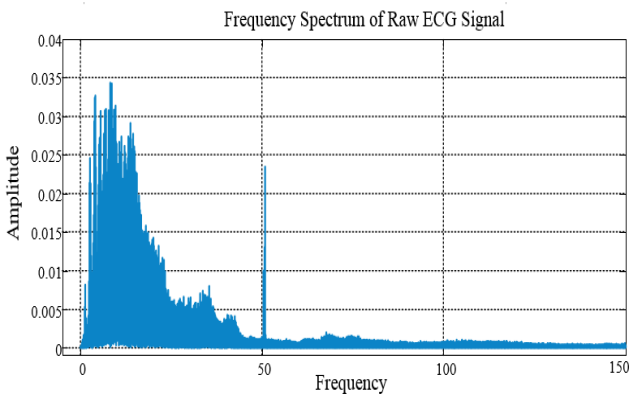

Fig.10: The frequency spectrum of the raw ECG signal

The 50 Hz noise and low frequency noises are visualised in Fig.10.

The bandstop filter with stopband between the frequency 45 and 55 Hz is used in order to remove the 50 Hz power line interference. The high pass filter with cut off frequency of 5 Hz is used in order to remove the low frequency baseline wandering noise. The low pass filter with cut of frequency of 100 Hz is used to remove the high frequency noise. The order of the filter is chosen as an optimum value of 100 because very higher order may attenuate the actual signal information along with the noise and cause the distortion of the signal, and lower value gives a poor noise reduction capability.

In addition to the FIR filter, a Savitzky-Golay filter has been implemented in order to smooth out the ripple with a wide frequency range from the signal. The Savitzky-Golay filters perform much better than standard averaging FIR filters, which tend to filter out a significant portion of the signal's high frequency content along with the noise [18].

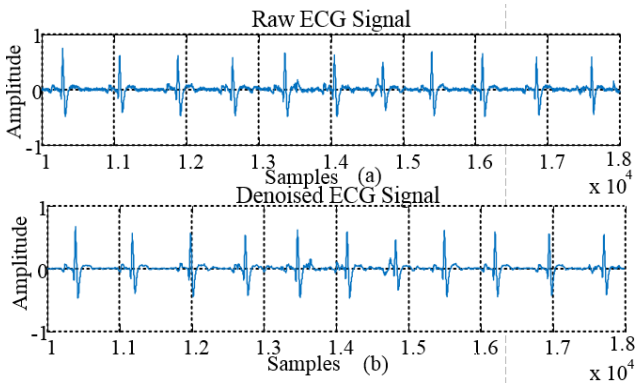

Fig.11: (a)-the raw ECG signal and (b)-the de-noised ECG signal

The signal obtained from the filter output is shown in Fig.11(b) which has clear shape in comparison of the raw ECG signal shown in Fig.11(a).

5.2 Feature Extraction

In this work, an algorithm has been developed in order to extract the R-R interval series for the purpose of mental stress analysis. At first, all of the R peaks available in the de-noised ECG signal are identified as shown in Fig.12(a) and then the time duration between the two consecutive R peaks are measured. Fig.12(b) shows the plot of the R-R interval series in seconds with respect to the number of interval.

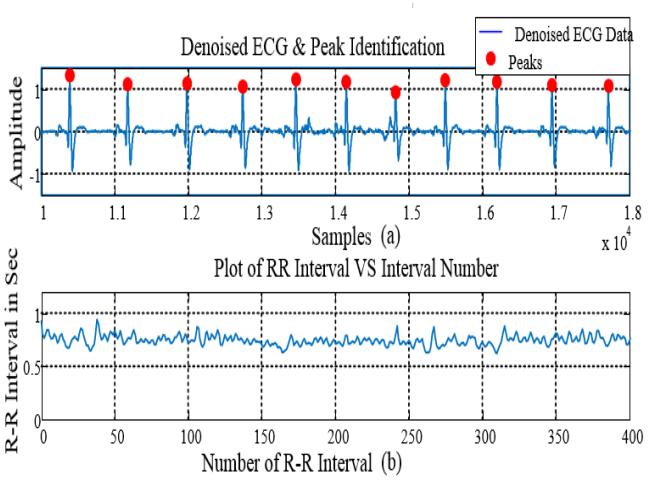

Fig.12: (a)-Peak Identification, and (b)-the R-R interval series.

5.2 Detrended Fluctuation Analysis

Detrended fluctuation analysis (DFA) is a method for determining the statistical self-affinity of a signal signal and useful in revealing the extent of long-range correlations in time series [19].This method has been successfully applied to a wide range of simulated and physiologic time series in recent years such as DNA sequences, neuron-spiking, human gait, and heart rate dynamics, sleep apnea [20], [21]. In many cases the DFA scaling exponent can be used to discriminate healthy and pathological data [22]. Detrended fluctuation analysis (DFA) measures the correlation within the signal. First, the RR interval time series is integrated.

$$y(k) = \sum_{j=1}^{k}\left(RR_j - \overline{RR}\right), k = 1, \ldots N; \qquad (4)$$

where $\overline{RR}$ is the average RR interval. Next, the integrated series is divided into segments of equal length n. Within each segment, a least squares line is

fitted into the data. Let y_n(k) denote these regression lines. Next the integrated series y(k) is detrended by subtracting the local trend within each segmented the root-mean square- fluctuation of this integrated and detrended time series is calculated by the following equation.

$$F(n) = \sqrt{\frac{1}{N}\sum_{k=1}^{N}(y(k) - y_n(k))^2} \quad (5)$$

correlations are divided into short-term and long-term fluctuations. The short-term fluctuations are characterized by the slope α_1 obtained within range $10 \leq n \leq 40$. Correspondingly, the short-term fluctuations are characterized by the slope α_2 obtained within range $70 \leq n \leq 300$ [21].

5.3 Recurrence Quantification Analysis

Recurrence quantification analysis (RQA) quantifies the small-scale structures of recurrence plots, which present the number and duration of the recurrences of a dynamical system [23]. The recurrence quantification analysis was developed in order to quantify differently appearing recurrence plots (RPs) based on the small-scale structures [24]. If only a time series is available, the phase space can be reconstructed by using a time delay embedding. In this approach, vectors

$$u_j = \left(RR_j, RR_{j+\tau}, \ldots\ldots\ldots\ldots RR_{j+(m-1)\tau}\right), \quad (6)$$

Where, $j = 1,2,\ldots\ldots\ldots\ldots, N-(m-\tau)$ and m is the embedding dimension and τ is the embedding lag. The vectors u_j then represents the RR interval time series as a trajectory in m dimensional space. In this paper, computation of RQA measures along the main diagonal of the RP was realized [25]. It expressed the time-dependent behaviour of these variables and obtained by computing the following parameters.

Recurrence rate (RR): It is a measure of density of recurrence points in the RP and defined as

$$RR = \frac{1}{(N-m+1)^2}\sum_{j,k=1}^{N-m+1} RP(j,k) \quad (7)$$

Determinism (DET): It is the ratio of recurrence points that form the diagonal structures to all recurrence points and reveal the signal repeats itself in adjacent trajectories:

$$DET = \frac{\sum_{lmin}^{lmax} lN_l}{\sum_{j,k=1}^{N-m+1} RP(j,k)} \quad (8)$$

Lmax: The maximal line length in the diagonal direction and expressed as

$$Lmax = max\left(\{l_i\}_{i=1}^{N_l}\right) \quad (9)$$

The entropy (ENTR): Entropy expresses the average information and complexity of RP with respect to diagonal lines. For example, the entropy of uncorrelated white noise is small, indicating low complexity.

$$ENTR = \sum_{l=l_{min}}^{l_{max}} n_l ln\, n_l \quad (10)$$

Laminarity (LAM): The ratio between the recurrence points forming the vertical structures and the entire set of recurrence points is called laminarity.

5.4 ANOVA Test

ANOVA (Analysis of Variance) is a statistical test to test whether there is a significant difference between two groups. ANOVA is a particular form of statistical hypothesis testing heavily used in the analysis of experimental data. Flow chart of performing ANOVA is given below:

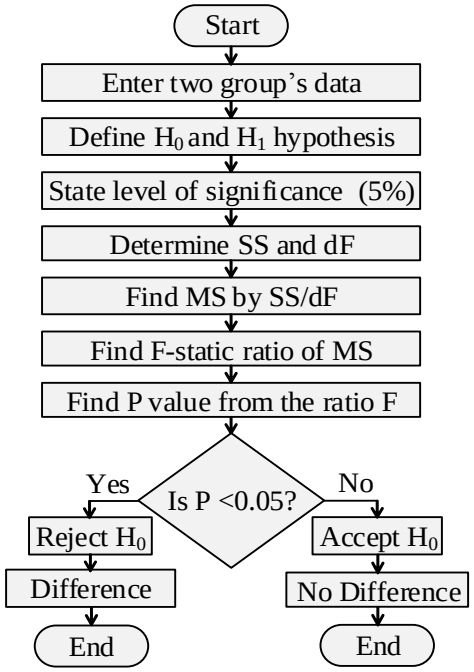

Fig.13: Flow chart showing the procedures of ANOVA test

6 Result

The value of DFA short term fluctuation, long term fluctuation, RR, DET, Lmax, ENTR, and LAM are tabulated below:

The evaluation parameters as shown in Table 1 and Table 2 are obtained by Detrended fluctuation analysis on RR intervals of two groups.

Table 1: DFA exponent of relaxed group

Sample Code	Short-term fluctuation Exponent, α1	Long-term fluctuation Exponent, α2
mah_01	0.6668	0.7954
soi_02	0.9123	0.6125
zia_03	0.9045	0.7153
far_04	0.8623	0.6665
sha_05	0.9312	0.8238
rat_06	0.7474	0.8054
azi_07	0.9826	0.8005
emo_08	1.0377	0.7068
nad_09	0.7891	0.8121
mah_10	0.8434	0.8122
eli_11	0.8269	0.7029
rob_12	0.8951	0.6655
hab_13	0.6111	0.6894
imr_14	0.9233	0.8557
far_15	0.8733	0.7185
sao_16	1.1231	0.7898
foi_17	1.0552	0.7505
apu_18	0.9578	0.9767

Table 2: DFA exponent of stress group

Sample Code	Short-term fluctuation Exponent, α1	Long-term fluctuation Exponent,α2
mas_01	0.9239	0.6892
rok_02	0.8142	0.6223
saz_03	0.9356	0.7047
mis_04	0.8310	0.7228
soj_05	0.7141	0.6874
jit_06	0.8001	0.8374
dip_07	0.6922	0.8025
foi_08	0.6673	1.1099
tou_09	0.7530	1.0621
jam_10	0.9429	0.6344
ala_11	1.0962	0.7219
tar_12	0.7821	0.8656
robi_13	0.7261	0.7744
miz_14	0.8334	0.8005
asr_15	0.7655	0.6274
oal_16	0.8960	0.9895
kri_17	0.9433	0.7042
bah_18	0.9202	0.8197

Table 3: RQA measures of relaxed group

Sample Code	RR $\times 10^{-4}$	DET $\times 10^{-5}$	L max	ENTR	LAM $\times 10^{-5}$
mah_01	1880	21	170	6.0606	42
soi_02	3109	22	104	6.4663	44
zia_03	175	26	14	3.7359	51
far_04	1822	24	77	5.9776	48
sha_05	1161	21	119	5.5874	42
rat_06	359	23	38	4.4430	45
azi_07	368	20	12	4.6745	39
emo_08	627	21	64	5.0994	42
nad_09	1244	27	19	5.4293	55
mah_10	895	25	77	5.2126	51
eli_11	1342	21	17	5.7915	42
rob_12	621	24	4	4.9959	48
hab_13	371	24	17	4.5150	47
imr_14	1630	24	158	5.8240	48
far_15	356	23	8	4.4747	47
sao_16	332	26	23	4.3322	51
foi_17	863	23	5	5.3618	44
apu_18	1215	26	12	5.4470	52

Table 4: RQA measures of stress group

Sample Code	RR $\times 10^{-4}$	DET $\times 10^{-5}$	L max	ENTR	LAM $\times 10^{-5}$
mas_01	271	28	2	4.2561	51
rok_02	233	23	2	4.1343	50
saz_03	2101	20	2	6.1962	41
mis_04	606	22	5	5.0769	44
soj_05	207	22	20	4.0015	45
jit_06	331	22	12	4.6441	41
dip_07	895	21	41	5.4085	43
foi_08	1152	25	59	5.4787	49
tou_09	1667	20	19	5.8397	40
jam_10	528	22	2	4.9353	43
ala_11	960	23	103	5.3739	46
tar_12	351	21	7	4.5393	44
robi_13	491	21	47	4.7516	42
miz_14	450	23	16	4.7098	47
asr_15	599	23	2	4.9801	47
oal_16	246	20	3	4.3665	41
kri_17	2868	21	2	6.4614	41
bah_18	418	24	32	4.5855	47

From table it is observed that numerical values of DFA short term fluctuation are same for two groups but long term fluctuations are different. Further ANOVA test is done for increasing assurance.

The RQA measures value shown in Table 3 and Table 4 are obtained by applying Recurrence Quantification Analysis on RR intervals of Relaxed and Stressed students. It can be seen from the table's numerical value that average value of RR, DET, ENTR, LAM almost same of two groups but Lmax value for relaxed group is higher than stressed group. To find out any difference ANOVA test is performed on above numerical data.

Table.5: ANOVA results of two groups for Methods DFA and RQA

Name of the parameters	probability	comment
DFA short term fluctuation	F=1.56(p>0.2201)	no difference of two groups
DFA long term fluctuation	F=0.45(p>0.506)	no difference of two groups
Recurrence rate (RR)	F=0.81(p>0.3751)	no difference of two groups
Determinism (DET)	F=2.43(p>0.1279)	no difference of two groups
Lmax	F=5.33(p<0.0268)	significance difference of two groups
The entropy (ENTR)	F=0.3(p>0.5864)	no difference of two groups
Laminarity (LAM)	F=1.9(p>0.1762)	no difference of two groups

From ANOVA Results shown in Table 5, it has been seen that there is no difference between two groups (relaxed and stress) of DFA parameters such as short and long term fluctuation are same for two groups. But in case of RQA parameters only Lmax measures are different of two groups but other RQA measures remain unchanged.

7 Conclusion

The paper aimed to the comparative study on DFA and RQA techniques to distinguish relaxed and stress group. The 30 min long ECG data recorded via the developed circuit undergoes the processing steps in order to be de-noised and to extract the required features. In this paper, we mainly work with the R-R intervals for heart rate variability complexity analysis using the DFA and RQA techniques. Short-term fluctuation Exponent, and long-term fluctuation exponent, maximal line length, recurrence rate, determinism, Shannon entropy, laminarity features are extracted for relaxed and stress group. Then ANOVA1 is applied to test whether there is a significant difference between two groups and from study it is concluded that RQA is better methods than DFA. For further study, other ECG features such as QRS complex, P-R interval, Q-T interval can be chosen for analysis and such analysis process can also be used for the study on various purposes such as the condition of people suffering from different heart related tasks and diseases.

References:

[1] J. Taelman, S. Vandeput, A. Spaepen, and S. V. Huffel, Influence of mental stress on heart rate and heart rate variability, *proc. of IFMBE,* 2008, pp. 1366–1369.

[2] V. Malhotra1, M. K. Patil, Mental stress assessment of ECG signal using stastical analysis of wavlet coefficient, *International Journal of Science and Research (IJSR)*, Vol.2, No.12, 2013, pp. 2060-2063.

[3] F. T. Sun, C. Kuo, H. T. Cheng, S. Buthpitiya, P. Collins, and M. Griss, Activity-aware mental stress detection using physiological sensors, *proc. of 2nd Int. ICST Conference*, CA, USA, Oct. 25-28, 2010.

[4] M. S. Chavan, R. A. Agarwala, M. D. Uplane, Interference Reduction in ECG using Digital FIR Filters based on rectangular window, *WSEAS Trans. on Signal Processing,* Vol.4, No.5, 2008, pp. 340-349.

[5] S. Rezk, C. Join, and S. E. Asmi, Inter-beat (R-R) intervals analysis using a new time dealy estimation technique, *proc. of 20th IEEE European Signal Processing Conference (EUSIPCO)*, Bucharest , Aug. 27-31, 2012.

[6] C. K. Karmakar, A. H. Khandoker, M. Palaniswami, Multi-scale tone entropy in differentiating physiologic and synthetic RR time series, *proc. of 35th Annual. International Conference, IEEE EMBS*, Japan, 3-7 July, 2013.

[7] S. Karpagachelvi, D. M. Arthanari, M. Sivakumar, ECG feature extraction techniques - a survey approach, *International Journal of Computer Science and Information Security,* Vol.8, No.1, 2010, pp. 76-80.

[8] K. Patil1, M. Singh, G. Singh, Anjali, N. Sharma, Mental stress evaluation using heart rate variability analysis: a review, *International Journal of Public Mental Health and Neurosciences,* Vol.2, No.1, 2015, pp. 9-16.

[9] M. Kumar, M. Weippert, R. Vilbrandt, S. Kreuzfeld, and R. Stoll, Fuzzy evaluation of heart rate Signals for mental stress assessment, *IEEE Trans. Fuzzy Systems*, Vol.15, No.5, 2007, pp 791 – 808.

[10] D. P. Goswami, D. N. Tibarewala, and D. K. Bhattacharya, Analysis of heart rate variability signal in meditation using second-order difference plot, *Journal of Applied Physics*, Vol.109, No.11, 2011, pp. 114703 - 114703-6.

[11] M. Kumar, S. Neubert, S. Behrendt, A. Rieger, M. Weippert, N. Stoll, K. Thurow, and R. Stoll, Stress monitoring based on stochastic fuzzy analysis of heartbeat intervals, *IEEE Trans. Biomedical Engineering*, Vol.20, No.4, 2012, pp. 746 – 759.

[12] M. K. Islam et al., Study and analysis of ECG signal using MATLAB & LABVIEW as effective tools, International Journal of Computer and Electrical Engineering, Vol.4, No.3, 2012, pp. 404-408.

[13] C. Kitchin and L. Counts, *A designer's guide to instrumentation amplifiers*, Analog Devices, Inc., U.S.A., 2006.

[14] J. G. Webster, *Medical instrumentation application and design*, John Wiley & Sons, New York, U.S.A.,2010.

[15] T. L. Floyd, *Electronics devices*, Pearson Education, Inc., New Jersey, U.S.A., 2005.

[16] P. J. Joshi, et al., ECG denoising using MATLAB, *International Journal of Scentific Engineering and Research*, Vol.4, No.5, 2013, pp. 1401-1405.

[17] M. S. Chavan, R. A. Agarwala, M. D. Uplane, Design and implementation of Digital FIR Equiripple Notch Filter on ECG Signal for removal of Power line Interference, *WSEAS Trans. on Signal Processing*, Vol.4, No.4, 2008, pp. 221-230.

[18] M. T. U. Zaman, et al., Comparative analysis of de-Noising on ECG signal, *International Journal of Emerging Technology and Advanced Engineering*, Vol.2, No.11, 2012, pp. 479-486.

[19] D. T. Schmitt, P. K. Stein, and P. C. Ivanov, Stratification pattern of static and scale-invariant dynamic measures of heartbeat fluctuations across sleep stages in young and elderly, *IEEE Trans. Biomedical Engineering*, Vol.56, No.5, 2009, pp. 1564-1573.

[20] C. -K. Peng, S. V. Buldyrev, S. Havtin, M. Simons, H. E. Stanley, and A. L. Goldberger, Mosaic organization of DNA nucleotides, *Physics Review E*, Vol.49, No.2, 1994, pp. 1685-1659.

[21] T. Penzel, J. W. Kantelhardt, L. Grote, J. H. Peter, and A. Bunde, Comparison of detrended fluctuation analysis and spectral analysis for heart rate variability in sleep and sleep apnea, *IEEE Trans. Biomedical Engineering*, Vol.50, No.10, 2013, pp. 1143-1151.

[22] J. Sun, Y. Tang, K. O. Lim, J. Wang, S. Tong, H. Li, and B. He, Abnormal dynamics of EEG oscillations in schizophrenia patients on multiple time scales, *IEEE Trans. Biomedical Engineering*, Vol.61, No.6, 2014, pp. 1756-1764.

[23] N. Marwan, and C. L. Webber, Jr., Mathematical and computational foundations of recurrence quantifications, in *Recurrence quantification analysis: theory and best practices*, Springer International Publishing, Cham, Switzerland 2015, chapter 1, pp. 29-43.

[24] G. Ouyang, X. Zhu, Z. Ju, and H. Liu, Dynamical characteristics of surface EMG signals of hand grasps via recurrence plot, *IEEE Journal of Biomedical and Health Informatics*, Vol.18, No.1, 2014, pp. 257-265.

[25] M. Niknazar, S. R. Mousavi, B. V. Vahdat, and M. Sayyah, A new framework based on recurrence quantification analysis for epileptic seizure detection, *IEEE Journnal of Biomedical and Health Informatics*, Vol.17, No.3, 2013, pp. 572-578.